10th Symposium on

High-Performance Marine Vehicles

HIPER'16

Cortona, 17-19 October 2016

Edited by Volker Bertram

TUHH
Technische Universität Hamburg-Harburg
Institut für Entwerfen von Schiffen und Schiffssicherheit
Schwarzenbergstraße 95 Gebäude C D-21073 Hamburg

TuTech
TUHH Technologie GmbH

Flagella Inspired Propulsion for AUVs

Marcis Eimanis, Institute of Mechanics, Riga/Latvia, marcis.eimanis@gmail.com
Janis Auzins, Institute of Mechanics, Riga/Latvia, auzinsjp@latnet.lv

Abstract

This paper presents an original design of an autonomous underwater vehicle where thrust force is created by the helicoidal shape of the hull. Propulsion force is created by counter-rotating bow and stern parts. The middle part of the vehicle contains all control mechanisms and communications that control the orientation of the vehicle. To solve the orientation problem special code is required using Arduino capabilities, adapting stabilization method of torques directed in opposite directions. The dynamics of AUV are simulated using multibody simulation software MSC Adams. Surrogate polynomial metamodels are created for simulation of water resistance forces and torques.

1. Introduction

Currently the most common underwater propulsion types are propellers. This propulsive force generator is also used for automated underwater vehicles, such as ships and other water vessels. As there has always been a tendency to borrow new mechanical ideas from nature and biological organisms, in past years many autonomous underwater vehicles (AUV) have been implemented according to the principle of fish-movement body/caudal fin propulsion. But in the world of bacteria, one of the ways to obtain locomotion is by rotating (like cork-screws) all parts of the body or flapping flagella, *Purcell* (1977), which is the simplest swimming method for a micro system. Bacteria Escherichia coli, *Spirochaetes* and many others move by rotating flexible parts of the body – one or many flagellas, *Eisenbach* (2011). At present there exist several scientific works on the simulation of flexible flagella motor-actuated bacteria dynamics and some physical experiments have been done with rotation of flexible helical tail constructions, *Flores (2005),* mainly using external magnetic field to drive them, *Ishiyama* (2000). Contra-rotating propellers (CRP) are well established as one of the most efficient technologies, *Caponnetto (2000)*, but in this paper we study contra-rotating parts of hull. So far there is no known functioning AUV that works on the basis of this principle. Only similarity in 2 dimensions from one point of view can be found in a robot based on the black ghost knife fish or *Apteronotus albifrons*, which uses inward counter-propagating waves for hovering or vertical swimming, *Curet (2011).* For human beings travel in a vehicle where all parts are rotating is not acceptable, but with the help of a rapid control system this is not an obstacle for AUV's.

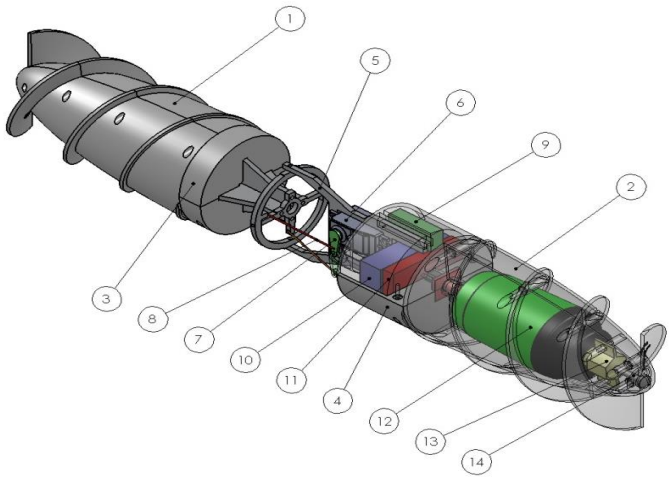

Fig.1: The structure of Durbis-2. 1, 2 – rear and front screw, 3 – mid-body front part, 4 – mid-body rear part, 5 – cross/ vector kite gimbal, 6 – servo, 7 – servo connector, 8 – shaft connecting connector and gimbal ring, 9 – analog signal receiver, 10 – battery, 11 – PDM type speed controller for DC motors, 12 – hull with DC motor and reducer, 13 – drive shaft, 14 – screw axis.

At Riga Technical University the design of AUV was developed using two reflection-symmetric parts with a helical shape. The parts are connected with motorized rotational joints. The vehicle contains a central part, Fig.1, with the hull built from elastic material. The central part contains a Cardan (universal) joint with two servomotors. The motorized Cardan joint implements the two-directional bending of the hull and allows maneuvering the vehicle. The direction control algorithm uses angular orientation sensor information. The AUV has 10 degrees of freedom.

2. Model design

The initial idea for the model came from the E. Coli bacteria that use external rotating body parts, called *flagellas*. Later we studied other bacteria that have the entire body in the form of a spiral (*Spirochaetes*) and move by a drilling motion of the body through a viscous environment. One approach to propelling microrobots in liquid environments is to mimic the flagella motor, which has been an object of investigation for several decades. In 1952 Taylor, *Taylor (1952)*, explored the swimming behavior of cells and bacteria, *Bell (2007)*. Retaining the idea that the entire body could rotate and generate drive force, a model design was developed for an underwater vehicle that consists of several (rather than one) rotating bodies. The initial conception was that one of the bodies will serve as a cargo space while the bow and the stern would serve for generating drive force. Since, generally, the entire body is used for generating drive force, as in the case of spiral bacteria, while the bow and the stern nevertheless are separately rotating parts that create driving (pushing and pulling) force, similar to E. Coli *flagellas*, then this idea of this model design can be considered to be a combination of both of the aforementioned bacteria. The cargo compartment must be static around its central axial axis (as far as possible, the top remains above and the bottom below), in order to successfully transport the cargo, therefore it is necessary to develop a method that would compensate the torques created by both threads on the middle body.

As for most water vehicles, the body form is similar to water organisms. Since least possible fluid flow resistance force is an important factor, it is necessary to adapt the vehicle form. To reduce drag of large submerged vehicles such as airships and submarines, their form is shaped according to proven physical principles. This can lead to unusual shapes which are impractical for submarines. To obtain a valid streamline shape for the hull, one way is to go back to basics, to find a solution which has developed naturally. Carmichael, *Carmichael (1966)*, tested streamlined torpedo shapes in drop tests in the Pacific Ocean. One shape, the "Dolphin", had half the drag of a conventional torpedo due to a long run of laminar boundary layer. Therefore, the accepted body form is an ellipse, the "ideal streamline form", *Joubert (2004)*, with the least pressure drag. Fig.2 shows that the bow is intended as parabolic, nevertheless, our vehicle is intended to be symmetric in order to avoid the necessity of reorienting the front for changing direction. This property would be very useful when moving in pipes where turning around is impossible. Since the body has a thread shape, the friction drag, which is one of the components considered in submarine form analysis, *Joubert (2004)*, will undoubtedly be large, but that is not an obstacle since the thread is the component that does the actual work. Therefore, in terms of choosing the form the most important goal is to obtain optimal streamlining.

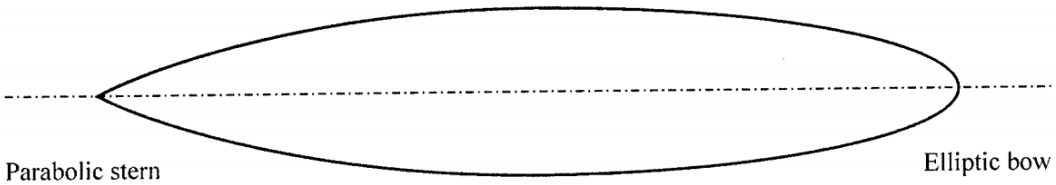

Fig.2: Ideal hull form, *Joubert (2004)*

Since the thread bodies we have introduced cannot be considered to be propellers, propeller theory cannot be directly applied to them. The *flagella* of a spermatozoid was taken as a point of reference in creating the thread geometry. The maximum angle of the undulation (angle of attack in propeller terminology) where optimal efficiency is achieved is $\theta_{max} \approx 40.06°$ (Fig.3), *Lauga (2013)*. However,

the bodies in our research are intended to be more similar to screws that drill the water, therefore another point of reference was the geometry of wooden screws. For wooden screws this thread angle in cross-section in relation to central axis (angle of attack) is ~15 degrees. Bearing this in mind, in the model this thread angle is ~22 degrees, with a pitch 106 mm. The thread body is covered by a double thread.

Fig.3: Angle of deformation of flagella.

The middle body serves both as a cargo compartment and implements the direction change function. It is intended to be flexible, allowing to change the driving force vector direction, changing the direction of the vehicle speed vector.

3. The control of helicoidal AUV with bending joints

The control principle of the AUV Durbis-2 is based on bending the Cardan joint in such a way that the rotation axis of the bow (front) screw would be oriented in the target direction. The rotation axis for tilting the bow screw from current position to the required direction is perpendicular to screw rotation axis unit vector *b* and to vector *a* from the center of vehicle to the target. The unit vector T of this finite rotation is equal to the cross product of both vectors, divided by the norm of vector ***a,***.Fig.4.

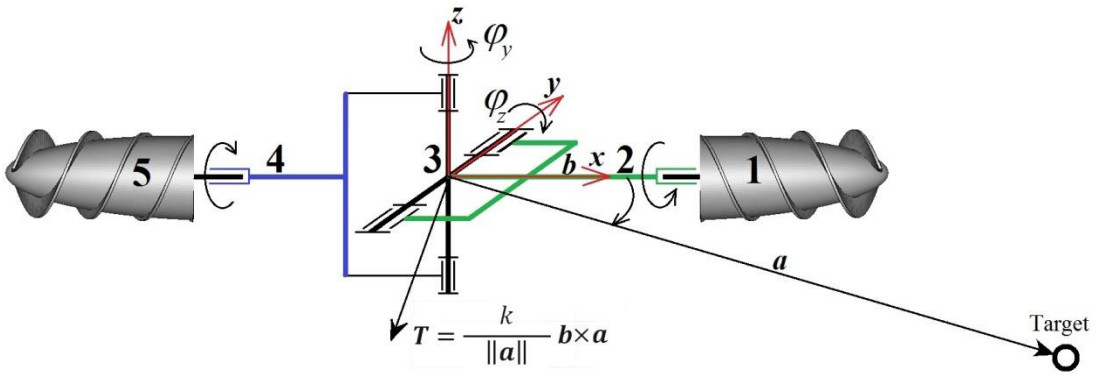

Fig.4: Kinematic diagram of Durbis-2. 1, 5 – bow and stern screws, 2 and 4 front and rear drive sections, 3 – Cardan journal cross (spider), φ_y, φ_z – tilt angles around Cardan joint axes, $\boldsymbol{a}$ – vector from the middle point of the Cardan joint to the target point, $\boldsymbol{b}$ – unit vector of bow screw rotation axis.

$$\boldsymbol{T} = \frac{1}{\|\boldsymbol{a}\|}\boldsymbol{b} \times \boldsymbol{a} \tag{1}$$

However, it should be taken into account that the control drive torques q_z and q_y are intrinsic, and the rear part of the vehicle will bend in opposite direction. We assume that the control system is equipped with sensors that give both current angles φ_y and φ_z of the servo-drives, as well as the projections of direction vector $\boldsymbol{a}$ on the axis of the central coordinate system (fixed on the Cardan journal cross). The control servo-drives can implement the required angle or rotation speed. In the case of speed control, a relatively simple control law can be implemented:

$$\begin{cases} \dot{\varphi}_y = -k_c arcsin(T_y) \\ \dot{\varphi}_z = k_c arcsin(T_z) \end{cases} \tag{2}$$

where k_c – constant coefficient. The control algorithm can use the vehicle linear velocity vector instead of axis vector ***b***. The main practical problem is the sensor system, which should include three-axis orientation sensors, because the middle part (middle body) can rotate around the longitudinal axis of vehicle. This fact makes simple manual control of the vehicle with two direction controllers impossible, because, due to rotation, the turn φ_z for the middle body is not always equal to yaw and φ_y is not always equal to pitch rotation.

4. Stabilization

In the case of Durbis-2, the stabilization problem applies specifically to the middle body where it is desirable to maintain the original orientation. Since the body includes the control system, in order to ensure its functioning, it is necessary to maintain the top part on top and the bottom part on the bottom. For the currently developed prototype Durbis-2, this middle body could easily turn upside down. The driving principle as such was not disturbed by this, however, the control system as impacted since all values become inverted, namely, the right side becomes the left side and the top becomes bottom. For the human brain it is difficult to quickly process such changes, therefore it is easy to lose control. To eliminate this drawback of Durbis-2, additional mass was added. In the new Durbis version it is planned to achieve this stabilization by compensating mutually opposed torques created by the thread bodies. A gyro-accelerometer with MEMS technology will help achieve this. This device will provide a direction for the Cardan cross coordinate system. For this purpose, an MPU-6050 gyro-accelerometer will be used, connected to an Arduino UNO microcontroller board. Our MEMS technology will electronically determine the model center coordinate system axis direction described by the angle $\Delta\varphi$, and it will be compensated with a control force created by one of the thread bodies (or both of them together). The idea was borrowed from the inverse pendulum stabilization problem described by the equation:

$$f(t) = k_1 x(t) + k_2 x'(t) + k_3(\theta(t) - \frac{\pi}{2}) + k_4\theta'(t) \qquad (3)$$

Since the model may rotate around the z- and y-axis without losing the top orientation of the middle body, then the compensation is necessary for rotation around the model longitudinal central axis z, or deviation from z-axis, Fig.5.

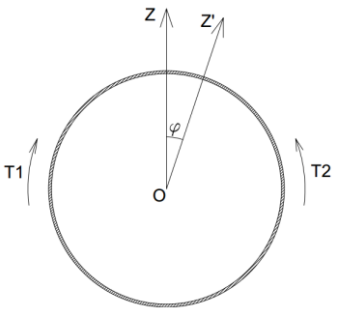

Fig.5: Schematic description of middle body stabilization (z-y cross-section)

This condition makes our problem 1 dimensional:

$$f(t) = k_1\varphi(t) + k_2\varphi'(t) \qquad (4)$$

The desired result is to maintain a single movement speed for the vehicle. Stabilization would be achieved by manipulating the projections of thread rotation speeds $\Delta\omega_i$ for each driving body on the longitudinal axis of cardan joint coordinate system:

$$\begin{cases} \Delta\omega_1 = k_1\varphi + k_2\dfrac{d\varphi}{dt} \\ \Delta\omega_2 = -k_1\varphi - k_2\dfrac{d\varphi}{dt} \end{cases} \quad (5)$$

To have a clearer view, it is only necessary to provide that the mid body does not turn around the central longitudinal x-axis, Fig.6. It can turn about other axis (y and z), while the vehicle makes movements to right-left, up-down. Thus we need only to attend so the Cardan journal cross y-axis, that at the beginning is at horizontal state and perpendicular to vertical z-axis, is always perpendicular to vertical z'-axis, which is given by sensor. This means that residual between vectors vertical direction of sensor and cross-joint vertical (originally) z-axis vector has to be projected on cross-joint axis, which primary was longitudinal axis.

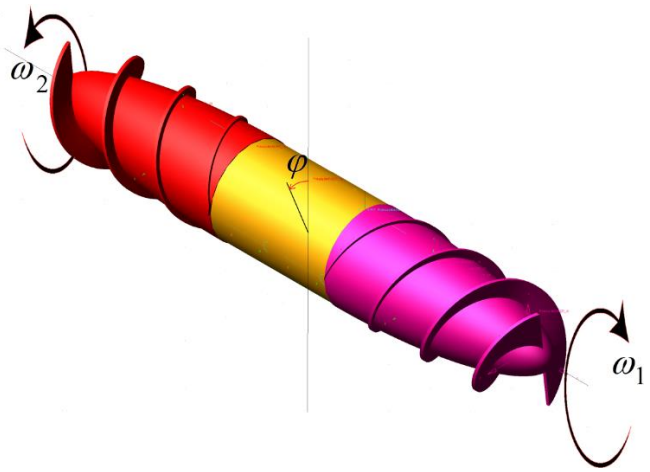

Fig.6: Schematic description of middle body stabilization

5. Creation of surrogate models of water resistance

Since it is practically impossible to simulate a moving mechanism with 10 degrees of freedom in CFD programs, taking into account full interaction between fluid and mechanism links, in practice the metamodeling (surrogate modeling) technology is broadly applied, *Carroll (2013)*. This requires the creation of simplified models of water resistance, obtained by planned experiments with CFD software. There are several good review papers that describe different aspects of surrogate modeling and advantages to numerous methods and they provided the background for choosing the appropriate method, *Forrester (2009)*, *Queipo (2005)*. The authors of *Carroll (2013)* used the classic Response surface method based on second order polynomial approximations of computer experiments with CFD software ANSYS FLUENT.

We used the software EDAOpt for design, analysis and optimization of computer experiments, created at Riga Technical University, *Auzins (2014)*. The polynomial surrogate models for water resistance forces $\boldsymbol{F}_i$ and torques $\boldsymbol{T}_i$ are created in the form

$$\boldsymbol{F}_i = -A_i^{\mathrm{T}}\boldsymbol{V}_i - \|\boldsymbol{V}_i\|B_i^{\mathrm{T}}\boldsymbol{V}_i \quad (6a)$$
$$\boldsymbol{T}_i = -C_i^{\mathrm{T}}\boldsymbol{\omega}_i - \|\boldsymbol{\omega}_i\|D_i^{\mathrm{T}}\boldsymbol{\omega}_i \quad (6b)$$

where $\boldsymbol{F}_i$ – column-vector of total water resistance force on the *i*-th body, $\boldsymbol{T}_i$ – column-vector of total water resistance torque acting about the center of mass of the *i*-th body, $\boldsymbol{V}_i$ - column-vector of translation velocity of center of mass of *i*-th body, $\boldsymbol{\omega}_i$ - column-vector of translation velocity of center of mass of *i*-th body, A_i, B_i, C_i, D_i – columns of coefficients, obtained by least-square approximation. All vector projections are calculated in body (moving) coordinate systems. When creating such surrogate models, the flow change from vehicle bending in the Cardan joint is not taken into account.

6. Simulation of rectilinear motion

Commercial CFD software ANSYS FLUENT, COMSOL Multiphysics, STAR-CD, Flow-3D and others provide limited capacity for modelling fluid-mechanism interaction dynamics. In these programs it is possible to insert into a fluid flow rigid bodies with all 6 degrees of freedom or constrain the motion excluding some translation or rotation degrees. The so-called General Moving Object (GMO) components can be of a mixed motion type, namely, have translational and/or rotational velocities that are coupled in some coordinate directions and prescribed in the other directions. A body-fixed reference system ("body system"), defined for each moving object, and the space reference system ("space system") are employed. Therefore, these rigid bodies can be coupled with the ground using rotational or translational joints. Unfortunately, it is not possible to connect two moving bodies among themselves using rotational joints.

To model rectilinear motion using software Flow-3D we used the following approach. Three main parts: bow (front) screw, middle body and stern (rear) screw are placed in alignment, allowing only rotation around longitudinal axis x. The middle body is standing still. In this model none of the three parts have any contact with each other and there are no contact forces or friction forces between them. An external torque Q around x-axis acts on the bow screw and the opposite torque –Q acts on the stern (right) screw. The mesh domain size in y and z directions was built in accordance with the recommendations given in *Watanabe (2003)* - approximately 1.4 times larger than the diameter of vehicle. We used the specified pressure conditions instead of wall-type boundary conditions. We used the idea that is applied in all wind tunnel experiments: the object may be moving through a stationary fluid, or the fluid may be flowing past a stationary object - these two are effectively identical since, in principle, it is only the frame of reference of the viewer which differs. In our simulations the vehicle is placed in such a way that its center of mass is fixed in the inertial coordinate system and the water flows past a stationary vehicle. CFD software calculates the fluid pressure and velocity in all mesh points as well as the total resistance forces and torques acting on all GMOs. The program also calculates the reaction forces and torques created by motion constraints. In our case there are three components of support reaction force and two components of reaction torque for each part of vehicle. The most important are the reaction force components in longitudinal direction, the other forces and torques are relatively negligible. In order to assume that the modelled movement is equivalent to a vehicle swimming with constant drive torques $q_1 = q_2 = Q$, it is necessary that the sum of reaction forces (called residual control x-force in the program Flow-3D, *Wei (2005)*) in longitudinal direction would be equal to zero, Fig.7:

$$R_{x1} + R_{x2} + R_{x3} = 0 \tag{7}$$

This condition can be satisfied only by experimentally determining the (external) drive torque value Q for each given fluid velocity value V_x, trying out different software input settings.

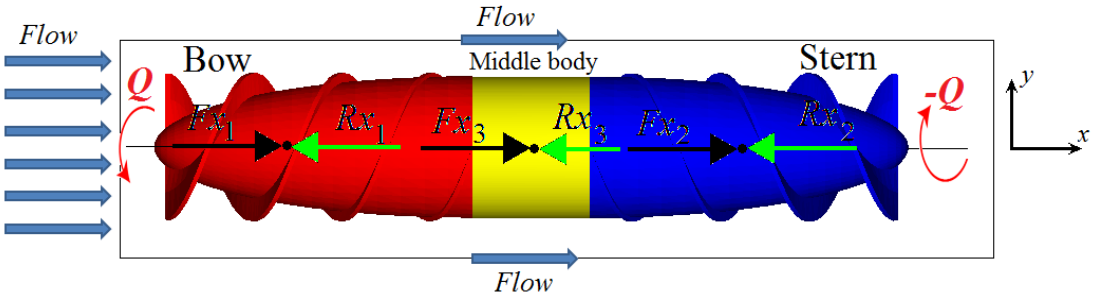

Fig.7: Top view of Durbis-2 in the finite volume mesh of the software Flow-3D

The Chen-Kim modification of Renormalized group (RNG) k-ε model, *Flow Science (2011)*, *Chen (1987)*, has been used for turbulence modeling with following coefficient values:

$$\left(\sigma_k, \sigma_\varepsilon, C_{\varepsilon 1}, C_{\varepsilon 2}, C_\mu, \beta\right) = (0.7194, 0.7194, 1.42, 1.68, 0.0845, 4.38, 0.012) \qquad (8)$$

Figs. 8 and 9 show the water streamlines and flow horizontal velocity contours for the fluid common velocity 0.6 m/s. The rear screw works inefficiently and pulls along the water behind it.

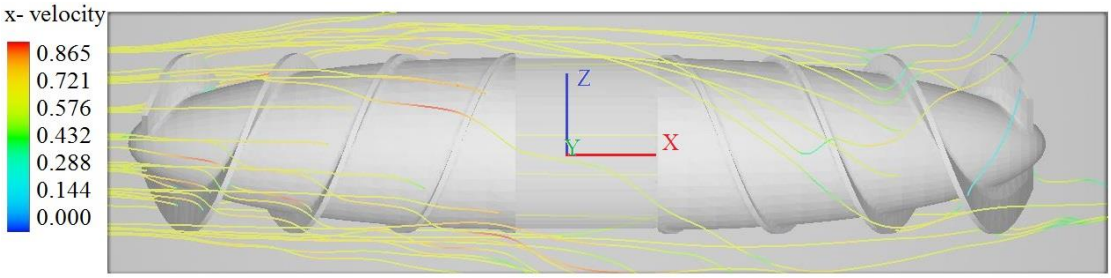

Fig.8: Water streamlines around Durbis-2. Velocity 0.6 m/s

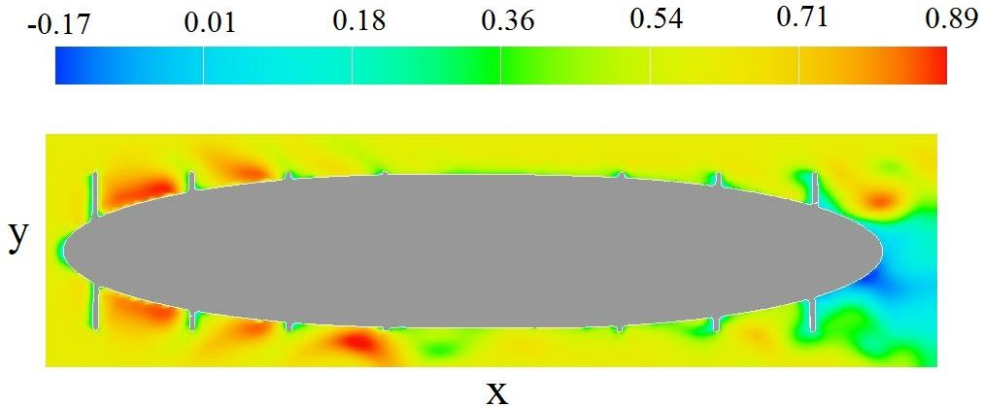

Fig.9: Fluid x-velocity contours in the middle section

Fig.10 shows the stabilization of rotational velocity of bow and stern screws and the oscillation of summary longitudinal reaction force for the given flow velocity 0.6 m/s and drive torque 0.146 Nm.

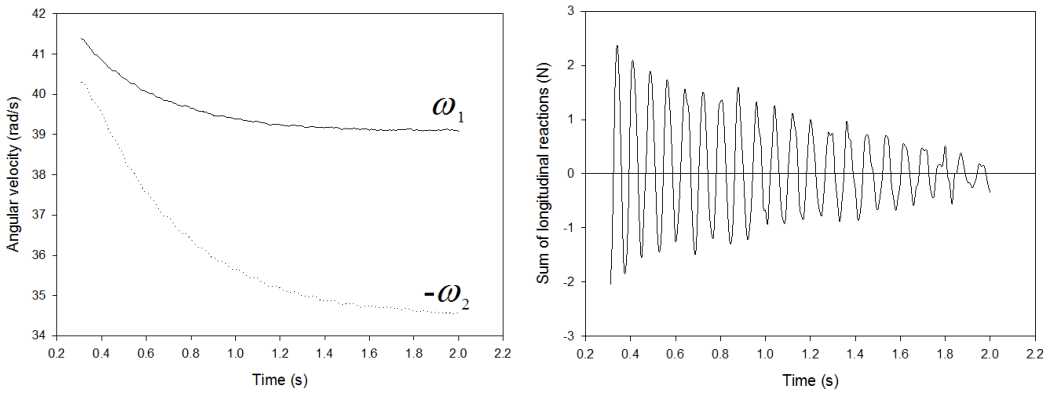

Fig.10: Stabilization of the screw rotation speed (left) and summary support reaction (right)

Fig.11 shows the approximated dependence of the drive torque on the velocity of rectilinear motion. Only four numerical experiments were used for obtaining this second order polynomial approximation. The adjusted R-square criterion value is 0.9997 and the value of the relative leave-one-out cross-validation, *Auzins (2014)*, is 5.3%, confirming the high adequacy of the approximation. The second order polynomial approximation contains a linear term that is insignificant in practice, see Pareto chart (*Auzins (2014)*, *Montgomery (2013)* p. 264), Fig.12.

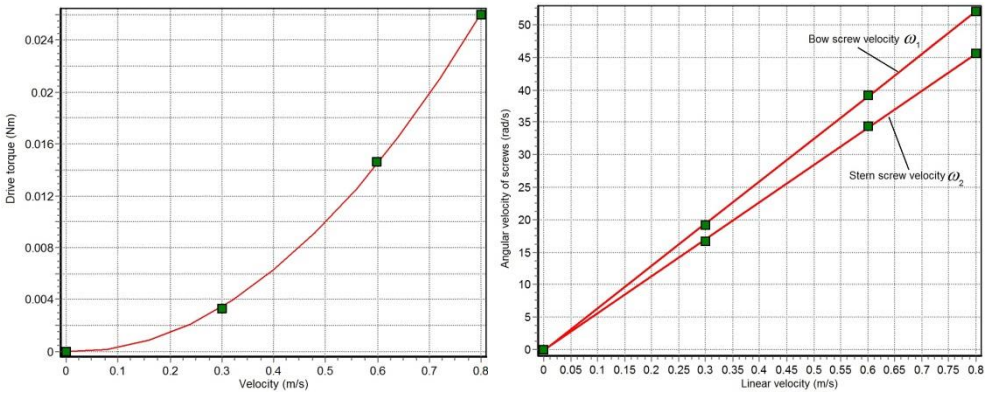

Fig.11: Approximate dependence of drive torque (left) and screw angular velocity (right) on the linear velocity of AUV

The right graph of Fig. 11 shows the approximated linear dependence between the velocity of rectilinear motion and angular velocities of bow and stern screws. The relative cross-validation error of approximation is about 1%. As can be seen, at equal (opposite) drive torques, the rear screw rotates significantly slower than the bow (front) screw. The fluid pressure and shear force analysis showed that the contribution of the rear screw in the creation of the thrust force is also significantly smaller.

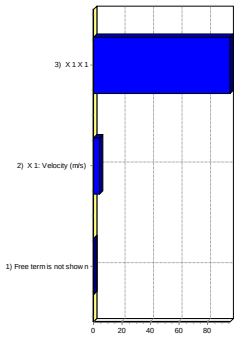

Fig.12: Pareto plot for the torque dependence approximation

The transverse motion velocity during vehicle turns is much smaller than the longitudinal speed. The surrogate water resistance force models were created by simulation of flow acting in the perpendicular direction. The water resistance torques around the transversal axis were calculated under the assumption that they are created by distributed pressure, proportional to squared velocity.

If the resistance force in the transverse direction can be approximated as $F_y = -k_y V_y^2$, then the simplest approximation for resistance torque for rotation around the perpendicular axis through middle point of a prolonged object will give $T_z = -\frac{k_y L^3}{32}\omega_z^2$, where Tz – the resistance torque around z-axis, ω_z – the angular speed of rotation around z-axis, L – the length of the body in longitudinal direction. Of course, this is a highly simplified approximation that does not take into account the interaction of rotation and translation movement, added mass effects, flow changes from the connected adjacent body parts.

7. Full dynamic simulation with MSC Adams

MSC Adams is world's most famous and widely used 3D Multibody Dynamics (MBD) software tool for dynamical analysis of mechanisms and machines, including mechanisms with rigid and flexible links, drive and control system. The mathematical model in the form of internal systems of differential-algebraic equations is built automatically according to the kinematic diagram which can be imported from any CAD software. Here we used MD Adams 2011, ID C00FD03A-BB49AF41.

The simulated mechanism contains 5 rigid-body links, connected with 4 rotational joints, Fig. 13 and 14.

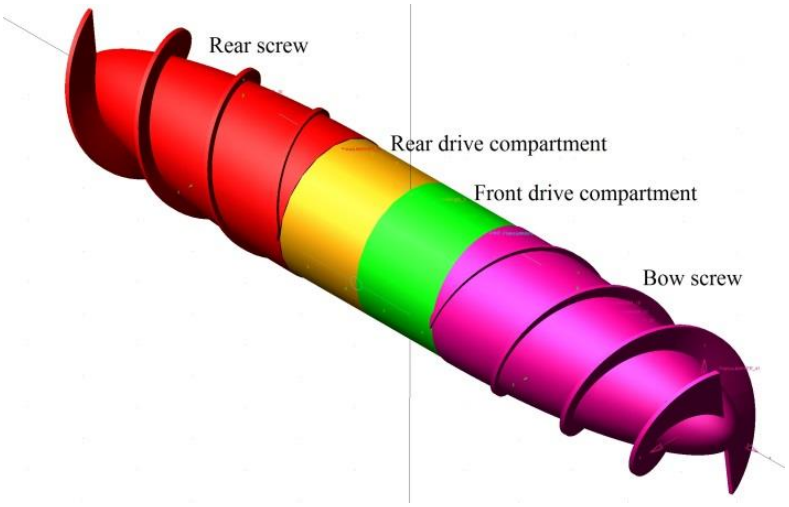

Fig.13: Durbis-2 in MSC Adams. Outside view. Cardan journal cross not shown

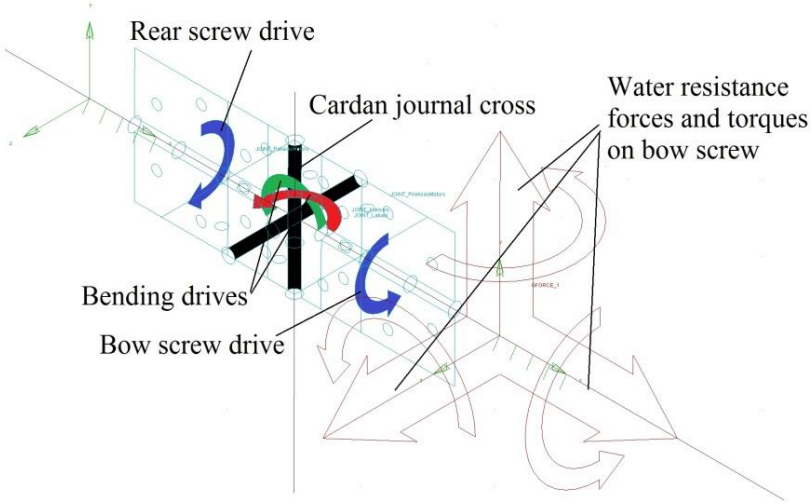

Fig.14: Durbis-2 in MSC Adams. The inner structure

Therefore, the model has 10 degrees of freedom. The water resistance forces and torques are given as external forces, using the created surrogate models and the possibilities of the function builder in MSC Adams. Fig.15 shows the "General force" property for the bow screw, which is in fact the realization of quadratic approximation of flow simulation results (6a, 6b).

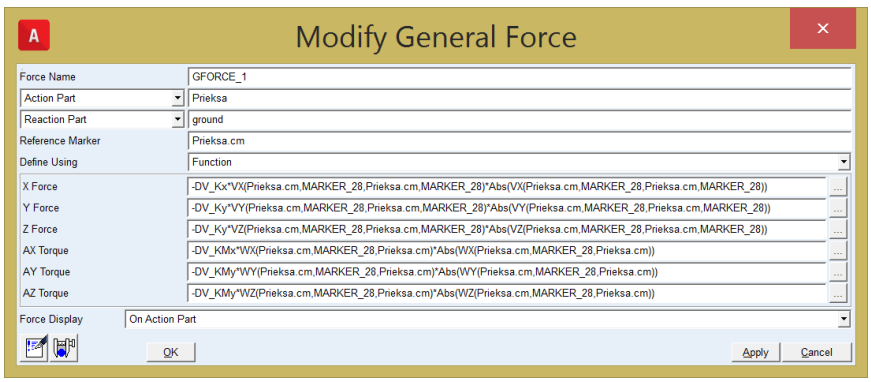

Fig.15: Water resistance surrogate model

The thrust and bending electro-drive dynamics were not simulated in detail. It was assumed that the thrust drives generate the necessary torque and orientation drives generate the necessary rotation speed. The angular velocity of bow and rear screws was varied in the range from zero to 20 RPM. When modelling rectilinear motion, at ±10 RPM the linear velocity of vehicle was obtained as about 0.6 m/s. Fig.16 shows the vehicle following a target, using an automatic control law (2). The spherical target moves in three dimensions according to sinusoidal law $x(t) = 0.7\sin(0.5t)$, $y(t) = 0.7\cos(0.5t)$, $z(t) = 0.46\sin(1.5t)$. The optimal value of the coefficient of control law (2) k_c =110 was found using computer experiments.

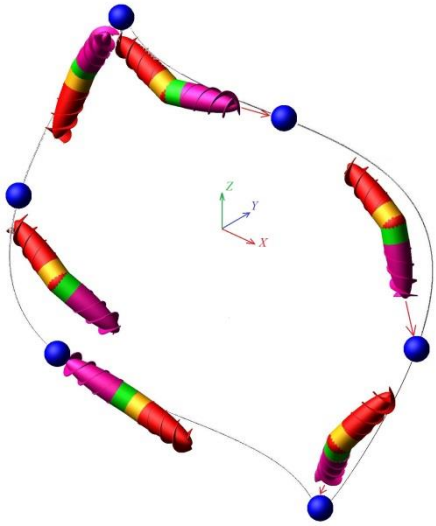

Fig.16: Following a moving target

8. Prototype of DURBIS-2 and validation

The physical prototype of the AUV DURBIS-2 was built in the master thesis of Marcis Eimanis, *Eimanis (2014)*, using CAD software SolidWorks and the Mass Portal 3D Printer Pharaoh Delta. The bow and stern screws were printed using PLA plastic. The screws are rotated with an LN22 Series electro drive individually connected to each screw (2 drives in total), using 7.4V Lipo battery, the reducer generates ~600 RPM and torque of about 0.06 Nm (controlled by *pulse-duration modulation*). Direction is controlled by 2 servo motors: Blue Bird High speed BSM-706, low profile (torque at 4.8V – 0.46 Nm; speed at 4.8V – 8 rad/s at no load). Low profile servomotors were deliberately selected to obtain additional free space for other components. The middle bending body consists of a Cardan-type cross construction, the material is 4mm thick EN-AW-5754 aluminum with an elastic silicone cover.

The middle body is water-proof and may be used as a "cargo compartment". The drive body is located on the central shaft that turns the spindle connected with the screw, causing it to rotate. The central shaft is fixed in a stationary position at the ends of the middle body. Model dimensions: total length 590mm, maximum diameter together with the screw 87.25mm, maximum diameter of hull 84mm, length of screw 190 mm, pitch of helix 106 mm. The range for the Cardan bending angles is ±30°. The prototype is not equipped with orientation sensors; therefore, it is controlled using a 40 MHz, 4.5-7.5V receiver placed in the vehicle body and a three-component control transmitter console. Due to the absence of middle body vertical orientation control and a sensor system for the prototype, an additional mass was placed in the lower part of the middle body to avoid its rotation around the longitudinal axis. This allows good remote control of the prototype. The remote control is possible at a distance of about 20 m and at about 2 m depth of submergence.

Fig.17: The prototype Durbis-2

The prototype Durbis-2 demonstrated very good maneuverability. The only measured parameters were linear velocity (about 0.6 m/s) and angular velocity of screws (about 600-700 RPM). This gives good agreement with simulation results from CFD and multibody dynamic simulation software. The real velocity and maneuverability of Durbis-2 is so high that the vehicle can move vertically and almost jump out of the water like a fish, Fig.18.

Fig.18: Durbis-2 „jumping" out of water

9. Conclusions

- Nature contains many organisms that provide new ideas for solving existing and future problems, particularly in regards to the microscopic world. Adapting microorganisms to technology allows solving problems from a new point of view and in greater detail.
- The numerical and physical simulation results have proved the functionality, maneuverability and energy efficiency of the proposed propulsion principle and control system. It must be noted that this principle can be used not only for underwater vehicles, but also for devices that move in granular, loose ground, as well as in pipes filled with fluid, including blood vessels. The experiment's measurements are compared with the results predicted using the computational model. The comparison shows that the model can predict with reasonably good accuracy the dynamic performance of the AUV with double helicoid hull shape.
- Further research should include more accurate analysis of the turbulence and cavitation effects.
- The stabilization problem is currently solvable by manipulating torques and thread body rotation speeds, each compensating the other, and retaining a stable movement speed as a result. This system employs MEMS technology together with Arduino programming capabilities, serving as the "brain" of the vehicle.

- Shape optimization of the hull and both screws would also be necessary. With the current design where the vehicle has almost completely symmetrical bow and stern parts, the stern screw has a mostly supportive function and the main thrust force is created by the bow screw. If the symmetry principle is abandoned, it would be possible to create a more energy-efficient shape for the double-helical vehicle.

References

AUZINS, J., EIMANIS, M. (2015), *Dynamical simulation and optimization of double-helical AUV*. VI International Conference on Computational Methods in Marine Engineering (MARINE 2015), Rome, Italy, 15-17 June 2015, pp. 1128-1139

AUZINS, J.; JANUSHEVSKIS, A.; JANUSHEVSKIS, J.; SKUKIS, E. (2014), *Software EDAOPT for experimental design, analysis and multiobjective robust optimization*, OPT-i Int. Conf. Engineering and Applied Sciences Optimization, Kos, pp. 101-123

BELL, D.J.; LEUTENEGGER, S.; HAMMAR, K.M.; DONG, L.X.; NELSON, B.J.; DONG D.X. (2007), *Flagella-like propulsion for microrobots using a magnetic nanocoil and rotating electromagnetic field*, IEEE Int. Conf. Robotics and Automation, pp.1128-1133

CAPONNETTO, M. (2000), *Optimisation and design of contra-rotating propellers*, SNAME Propellers/Shafting Symp., Virginia Beach, pp.3.1-3.9

CARMICHAEL, B.H. (1966), *Underwater vehicle drag reduction through choice of shape*, AIAA Paper 66-657

CARROLL, J.; MARCUM, D. (2013), *Developing a surrogate-based time-averaged momentum source model from 3D CFD simulations of small scale propellers*, World Congress on Engineering, London, pp.1622-1627

CHEN, Y.S.; KIM, S.W. (1987), *Computation of turbulent flow using an extended k-ε turbulence closure model*, NASA Report, CR 179204

CURET, O.M.; PATANKAR, N.A.; LAUDER, G.V.; MACIVER, M.A. (2011), *Aquatic maneuvering with counter-propagating waves: a novel locomotive strategy*, J. R. Soc. Interface 8, pp.1041-1050

EIMANIS, M. (2014), *Development of new type propulsion device for underwater vehicles*, Master thesis, Riga Technical University, https://ndr.rtu.lv/lv/view/11681/

EISENBACH, M. (2011), *Bacterial Chemotaxis*. In: eLS. John Wiley

FLORES, H.; LOBATON, H.;, MÉNDEZ-DIEZ, E.S.; TLUPOVA, S.; CORTEZ, R. (2005), *A study of bacterial flagellar bundling*, Bulletin of Mathematical Biology 67, pp.137-168

FORRESTER, A.;, KEANE, A. (2009), *Recent advances in surrogate-based optimization*, Progress in Aerospace Sciences 45, pp.50-79

ISHIYAMA, K.; ARAI, K.I.; SENDOH, M.; YAMAZAKI, A. (2000), *Spiral-type micromachine for medical applications*, Int. Symp. Micromechatronics and Human Science

JOUBERT, P.N. (2004), *Some aspects of submarine design. Part 1*, DSTO Platforms Sciences Laboratory, pp.15-26

LAUGA, E.; ELOY, C. (2013), *Shape of optimal active flagella*, J. Fluid Mechanics 730

MONTGOMERY, D.C. (2013), Design and Analysis of Experiments, John Wiley & Sons

PURCELL, E. M. (1977), *Life at Low Reynolds Number*, American J. Physics 45, pp. 3-11

QUEIPO, N.V.; HAFTKA, R.T.; SHYY, W.; GOEL, T.; VAIDYANATHAN, R.; TUCKER, P.K. (2005), *Surrogate-based analysis and optimization*, Progress in Aerospace Sciences 41, pp.1-28

TAYLOR, G. (1952), *The action of waving cylindrical tails in propelling microscopic organisms*, Proc. Royal Society of London Series A-Mathematical and Physical Sciences 211, pp. 225-239

WATANABE, T.; KAWAMURA, T.; TAKEKOSHI, Y.; MAEDA, M.; RHEE, S.H. (2003), *Simulation of steady and unsteady cavitation on a marine propeller using a RANS CFD code*, 5th Int. Symp. Cavitation (CAV2003), Osaka, pp.1-4

WEI, G. (2005), *A fixed-mesh method for general moving objects in fluid flow*, Modern Physics Letters B, Vol. 19, Issue 28-29, pp.1719-1722